J Solid State Electrochem (2016) 20:1855–1863
DOI 10.1007/s10008-016-3151-5

ORIGINAL PAPER

Enhanced electrochemical performance of carbon-coated $LiMPO_4$ (M = Co and Ni) nanoparticles as cathodes for high-voltage lithium-ion battery

P. Ramesh Kumar[1] · V. Madhusudhanrao[2] · Nageswararao B[2] · M. Venkateswarlu[3] · N. Satyanarayana[1]

Received: 11 July 2015 / Revised: 4 February 2016 / Accepted: 8 February 2016 / Published online: 19 February 2016

Abstract Olivine $LiMPO_4$ (M = Co and Ni) nanoparticles have been synthesized by the polyvinylpyrrolidone (PVP) assisted polyol method and adopted the resin coating process for carbon coating on the surface of the nanoparticles. The X-ray diffraction (XRD) and Fourier transform infrared (FTIR) spectroscopy studies confirmed the phase and structural co-ordination of bare and carbon-coated $LiMPO_4$ (M = Co and Ni) nanoparticles, respectively. The formation of uniform carbon layer of nanometer-measured thickness over nanoparticles is confirmed by the high-resolution transmission electron microscopy (HRTEM) and energy-dispersive X-ray spectroscopy (EDS). Wagner's polarization study explains an improved electronic transport number (t_e) for carbon-coated $LiMPO_4$ (M = Co and Ni) cathodes as compared to bare samples. The electrochemical study of the Li-ion cells shows the first cycle discharge capacities of 180 and 97 mAh/g at 0.1 C for the cathodes $LiCoPO_4$/C and $LiNiPO_4$/C, respectively, which is an improvement of 21.2 and 25.8 % as compared to bare samples. The enhancement of electrochemical performance of the cells is attributed to the improved electronic properties of cathode materials due to the presence of carbon on the surface of nanoparticles.

Keywords Resin coating process · Carbon coating · Lithium metal phosphates · Cathode · Li-ion battery · Capacity

✉ Nageswararao B
vallabhaneni999@yahoo.com

[1] Department of Physics, Pondicherry University, Pondicherry 605014, India

[2] Vignan's University, Vadlamudi, Andhra Pradesh 522 213, India

[3] Amara Raja Batteries Ltd., Karakambadi, Andhra Pradesh 517 520, India

Introduction

Rechargeable lithium-ion batteries (LIBs) with high energy densities and high voltages are in great demand for portable electronic devices, such as smartphones, tabs, etc. And, they are also emerging applications, such as electric vehicles (EVs) and hybrid electric vehicles (HEVs) due to smaller footprint and quick charging characteristics of technology [1, 2]. Today, the cobalt oxide and iron phosphate chemistries are playing dominant role, respectively, in the portable electronic devices and automotive applications. The cobalt oxide chemistry is unsafe and expensive, whereas the iron phosphate-based chemistry is safe and has high operating potential relatively [3]. Recently, efforts have been intensified to explore alternative cathode materials with cost-effective and enhanced safety. Among the reported chemistries of cathode materials, the olivine-structured $LiMPO_4$ (M = Fe, Mn, Co, and Ni) cathode materials are favorable for high power density applications mainly due to their high redox potentials [4 to 5 V vs. Li^+/Li], high structural stability for repeated cycling, and enhanced safety [4–6]. However, the low electronic and ionic conductivities of $LiMPO_4$ (M = Fe, Mn, Co, and Ni) cathode materials have limited their practical applications. The poor electrical properties of cathode materials are due to the defect association effect, which has a strong impact on material transport properties [7]. In order to improve the electrical properties of cathode materials, several approaches, such as reducing the particle size from micro to nanosize, doping, surface treatment, etc., have been attempted [8–11]. The nanosize particles in principle provide shorter diffusion lengths for Li-ions and high surface area contact with electrolyte for electron transfer,

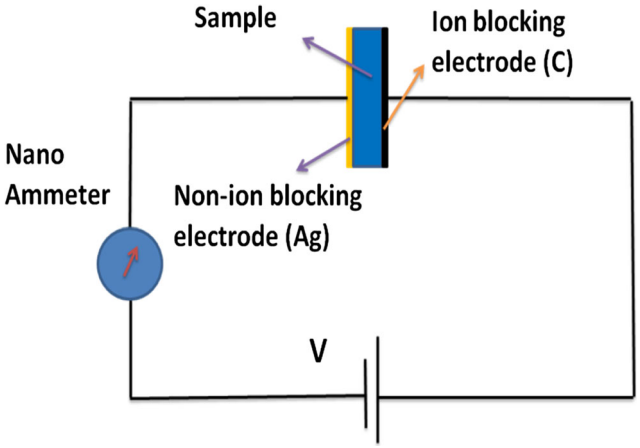

Fig. 1 Schematic representation of the Wagner's polarization method

leading to an improved battery performance [2, 11, 12]. Malik et al. reported that the small size particles exhibit improved ionic diffusivity [7]. Another novel approach was the surface treatment of particles with conductive agents, such as carbon, polypyrrole (Ppy), etc., which is effective in enhancing the electron kinetics of the electrode. The most extensive and successful research is the special carbon coating on the cathode materials of $LiMPO_4$ (M = Fe, Mn, Co, Ni, etc.) and has achieved a significant improvement in their electrochemical performance [8, 13–24]. Recently, the $LiFePO_4$/C nanocomposite cathode material prepared by a two-step method exhibited a higher discharge capacity [25]. As reported by Ying et al., the carbon-coated $LiNiPO_4$ cathode exhibited higher capacity and good rate capability as compared to bare sample [26]. Very recently, the carbon-coated $LiCoPO_4$ particles synthesized by microwave-assisted path exhibited good electrochemical performance [27]. Ramesh et al. has studied the effect of carbon coating on the surface of $LiMnPO_4$ nanorods and observed an improvement in the battery performance compared to bare sample [28].

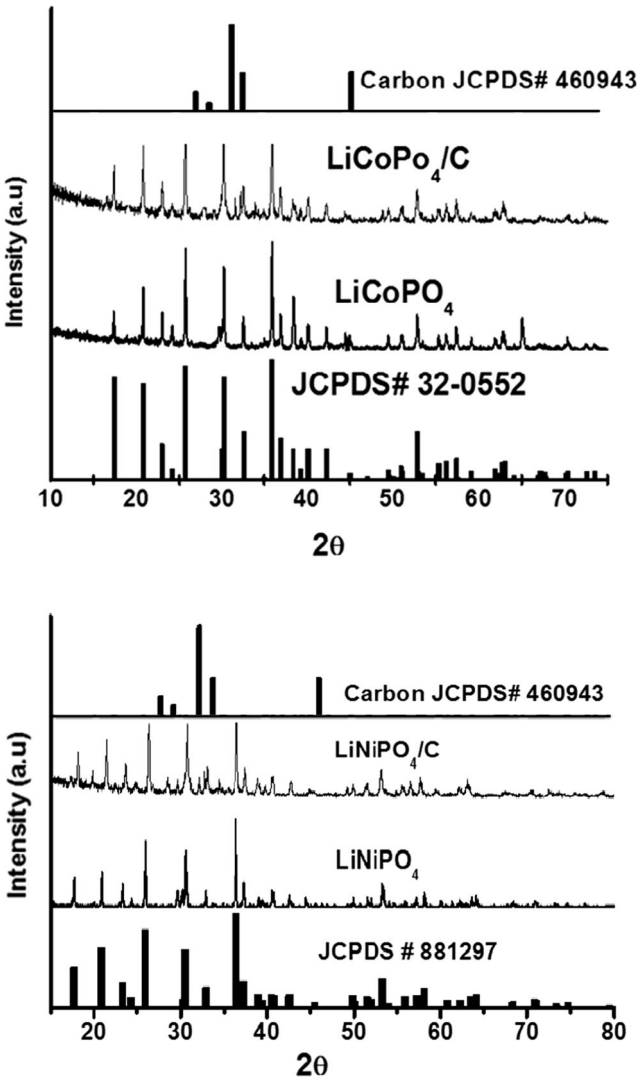

Fig. 2 XRD patterns of the pure and carbon-coated $LiCoPO_4$ and $LiNiPO_4$ nanoparticles

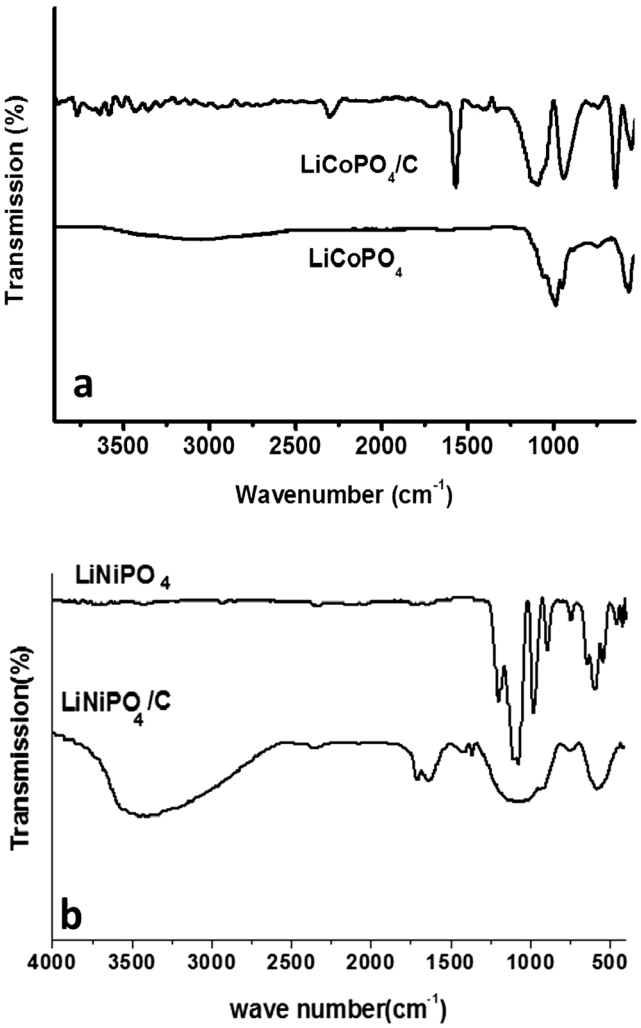

Fig. 3 FTIR spectra of pure and carbon-coated **a** $LiCoPO_4$ and **b** $LiNiPO_4$ nanoparticles

In this paper, we have made an attempt to prepare pure and carbon-coated $LiMPO_4$ (M = Co and Ni) nanoparticles by polyol and novel resin coating processes, respectively, and study their efficiency as positive electrode (cathode) in LIBs. The synthesized cathode nanoparticles were subjected to the characterization by XRD, FTIR, and TEM-EDS to evaluate the phase purity, structure, particle size, and the presence of conductive coating on the surface of the particles, respectively. Further, the Wagner's polarization technique has been used to evaluate the transport number of the bare and coated samples. The Li-ion cells (2032) have been fabricated with bare and carbon-coated $LiMPO_4$ (M = Co and Ni) cathode materials, and the electrochemical study has been carried out in the potential range 4.5 to 5.0 V, at room temperature.

Experimental

The $LiMPO_4$ (M = Co and Ni) nanoparticles have been synthesized by the polyol process with respective precursors, lithium acetate, metal acetates, and ammonium di-hydrogen phosphate materials and were dissolved in ethylene glycol. The polyvinylpyrrolidone $[(C_6H_9NO)_n$, MW 40,000)] is used as surfactant and added to the glycol solution, in order to optimize the particle size and also to avoid agglomeration of nanoparticles. The mixture has been heated up to 190 °C under constant stirring for 2 h to form a precipitate and then separated from solution by centrifugation. The resultant precipitate has been rinsed several times with de-ionized water followed by acetone and then dried out at 55 °C for 12 h. The dried powder was further calcined at 600 °C for 3 h to form pure crystalline phase of $LiMPO_4$ (M = Co and Ni) nanoparticles.

In order to coat thin carbon layer over $LiMPO_4$ (M = Co and Ni) nanoparticles, novel resin coating process has been

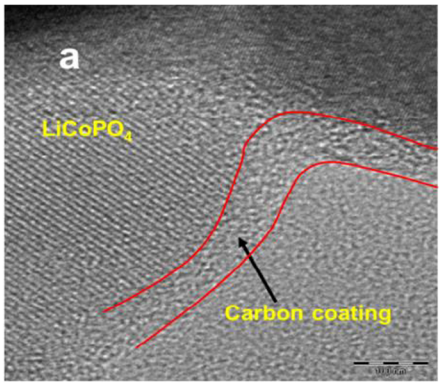

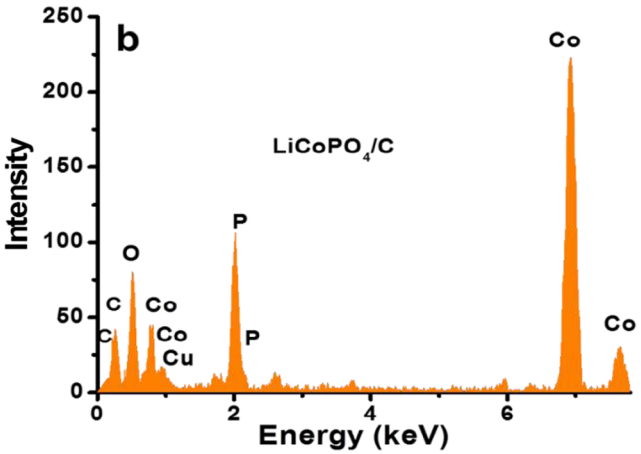

Fig. 5 **a** HRTEM image and **b** EDS spectrum of the carbon-coated $LiCoPO_4$ nanoparticles

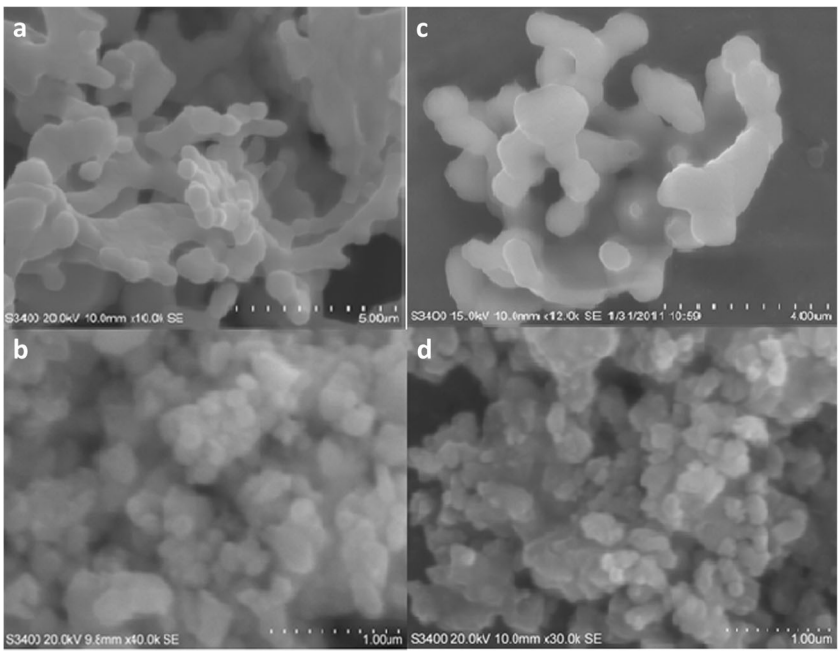

Fig. 4 SEM images of the **a** pure $LiCoPO_4$, **b** carbon-coated $LiCoPO_4$, **c** pure $LiNiPO_4$, and **d** carbon-coated $LiNiPO_4$ nanoparticles

deployed. The acrylic acid and ethylene glycol, for 2 % carbon coating, are mixed with well-dispersed $LiMPO_4$ (M = Co and Ni) nanoparticles under constant stirring. The resultant mixture has been heated to 80 °C to form a resin on the surface of the nanoparticles. Further, the obtained powder has been calcined at 350 °C to form thin carbon layer over the $LiMPO_4$ (M = Co and Ni) nanoparticles. The prepared samples have been subjected to characterization to understand the structural, particle morphology, and electrical properties by deploying XRD, FTIR, scanning electron microscopy (SEM), TEM, and Wagner's polarization techniques. The XRD patterns have been recorded for all the prepared samples using the PANanalyticalXpert Pro X-ray diffractometer with Cu $K\alpha$ radiation of wavelength 1.5418 Å and scanned in the range 10°–80°. The FTIR spectra have been recorded on thin transparent pellet samples using the FTIR spectrometer (Shimadzu FTIR 8300/8700) in the range of 4000–400 cm^{-1} with resolution of 2 cm^{-1} for 20 scans. The particle size, distribution, and morphology of the samples have been examined on SEM (Hitachi S3400N). Further, the presence of carbon in the carbon-coated $LiCoPO_4$ nanoparticles has been confirmed using the high-resolution transmission electron microscopy (HRTEM: JEOL 2010F) with 200 kV as an operating voltage. The number of transported electrons and ions in the pure and carbon-coated $LiMPO_4$ (M = Co and Ni) nanoparticles has been measured using Wagner's polarization method, and the schematic diagram of the Wagner's polarization method is shown in Fig. 1. As shown in Fig. 1, the sample (pure and/or carbon-coated $LiMPO_4$ (M = Co and Ni) nanoparticles) has been placed between two electrodes (ion blocking and non-ion blocking) and applied a DC potential. The current measured is a function of time for a fixed applied DC potential. The initial observed current is called total current (i_T), and it is found to decrease with time and then reaches to saturation after some time. The decrease of current (i_T) with time may be due to the polarization of ions at the ion blocking electrode. The extrapolation of saturation current curve to y-axis gives the electronic current (i_e) [29].

The total current (i_T) in any given system is the sum of the current due to ions (i_i) and the current due to electrons (i_e)

$$i_T = i_i + i_e \tag{1}$$

The ionic current of each sample can be obtained using the relation [$i_i = i_T - i_e$] from Eq. (1) and also evaluated the total current (i_T) and electronic current (i_e).

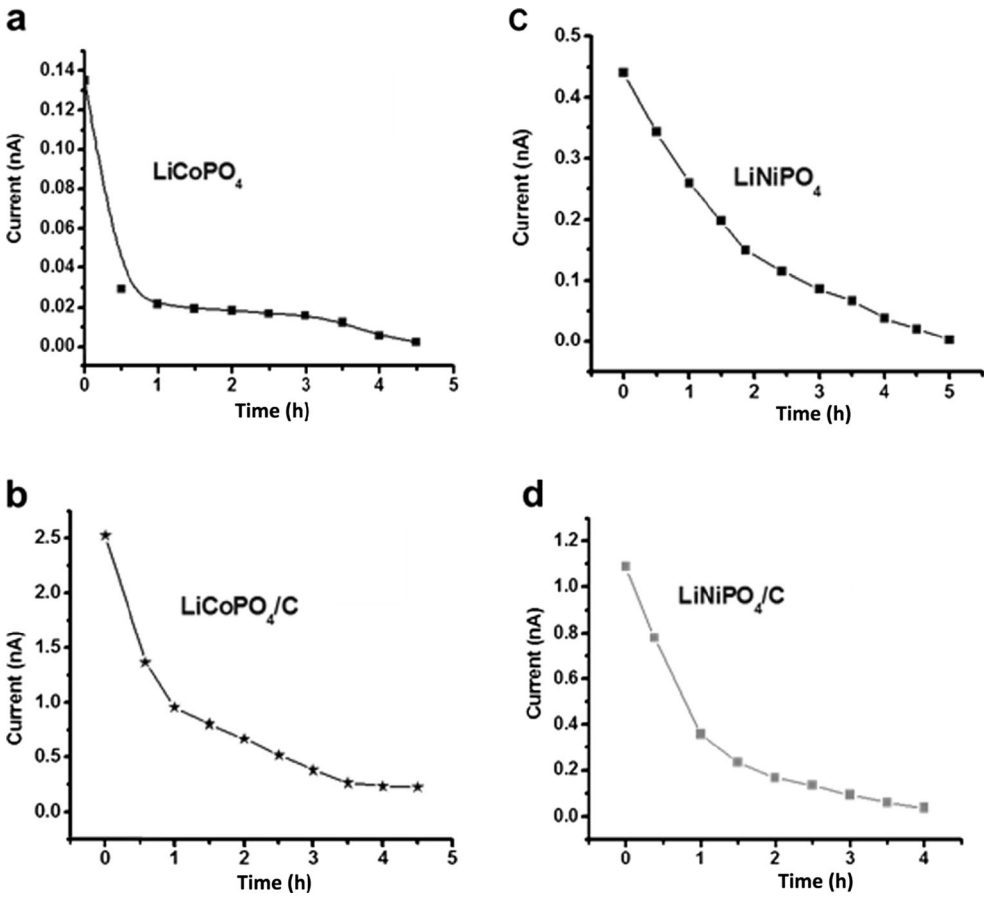

Fig. 6 Current versus time plots of **a** pure $LiCoPO_4$, **b** carbon-coated $LiCoPO_4$, **c** pure $LiNiPO_4$, and **d** carbon-coated $LiNiPO_4$ nanoparticles

The ionic (t_i) and electronic (t_e) transport numbers of each sample can be calculated using Eqs. (2) and (3).

$$\text{Ionic transport number } (t_i) = i_i/i_T \quad (2)$$

$$\text{Electronic transport number } (t_e) = i_e/i_T \quad (3)$$

From Eqs. (1), (2), and (3), the total (i_T), ionic (i_i), and electronic current (i_e) values will be calculated.

The CR2032 coin-type Li-ion cells have been assembled in an argon-filled glove box (Vacuum Atmospheres Co. (VAC), USA). The lithium metal is used as negative electrode, and the pure and carbon-coated $LiMPO_4$ (M = Co and Ni) are used as positive electrode (cathode). The positive electrode consists of 80 wt% active materials, 15 wt% conductive carbon (Super P, Timcal), and 5 wt% of poly(vinylidene fluoride) (PVDF) binder in N-methyl pyrrolidone (NMP) solvent. A Celgard-2340 μ porous three-layered polymer (PP/PE/PP) membrane has been used as separator. The separator is placed in between the two electrodes subjected to soaking in an electrolyte solution of 1 M $LiPF_6$ in EC/DMC (1:1 *v*/v). The electrical tests are carried out galvanostatically on the fabricated lithium-ion cells using multi-channel battery tester (ARBIN BT2000) at a current load of 0.1 C, in the potential range 4.0–5.3 V (vs. Li/Li^+), at ambient conditions.

Results and discussion

Structural analysis

Powder XRD patterns of the bare and carbon-coated $LiMPO_4$ (M = Co and Ni) samples and also the Joint Committee on Powder Diffraction Standards (JCPDS) data are shown in Fig. 2. From Fig. 2, the formation of crystalline phases of $LiCoPO_4$ and $LiNiPO_4$ could be confirmed by comparing the observed XRD patterns of the test samples with respective JCPDS data. The average crystallite size of the samples has been calculated using Scherrer's formula and is found to be 60 nm for both pure and carbon-coated $LiMPO_4$ (M = Co and Ni) nanoparticles. The XRD patterns of carbon-coated $LiMPO_4$ (M = Co and Ni) samples have showed two extra peaks at 28° and 31.5°, which correspond to the crystalline phase of carbon in the samples. Hence, XRD results confirmed the formation of crystalline phases of $LiCoPO_4$ and $LiNiPO_4$ and also the presence of carbon in the carbon-coated $LiMPO_4$ (M = Co and Ni) particles.

The FTIR spectra of bare and carbon-coated $LiMPO_4$ (M = Co and Ni) samples are shown in Fig. 3. From Fig. 3a, b, the FTIR spectra of the bare and carbon-coated $LiMPO_4$ (M = Co and Ni) nanoparticles show IR bands at 950 and 1070 cm^{-1}, which are due to symmetrical and asymmetrical stretching vibrations of PO_4^{-3}, respectively. The IR bands between 641 and 480 cm^{-1} are due to the asymmetric bending modes of O–P–O [28]. Thus, FTIR results have confirmed the presence of PO_4^{-3} structure in the pure and carbon-coated $LiMPO_4$ (M = Co and Ni) nanoparticles.

The broad peak observed from 3582 to 3236 cm^{-1} in pure $LiMPO_4$ (M = Co and Ni) samples is assigned to the stretching vibrations of O–H groups (due to the adsorbed moisture) [30]. The carbon-coated $LiMPO_4$ (M = Co and Ni) nanoparticles have showed an extra bands at 1728 and 1621 cm^{-1}, which are attributed to the symmetrical stretching vibrations of C–O and C–C, respectively [31]. Also, the IR band observed at 745 cm^{-1} correspond to the P–O–C symmetric stretching vibrations, which further confirmed the presence of carbon in the carbon-coated $LiMPO_4$ (M = Co and Ni) nanoparticles [31].

Morphology analysis

Figure 4 shows the SEM images of both bare and carbon-coated $LiMPO_4$ (M = Co and Ni) nanoparticles. From SEM

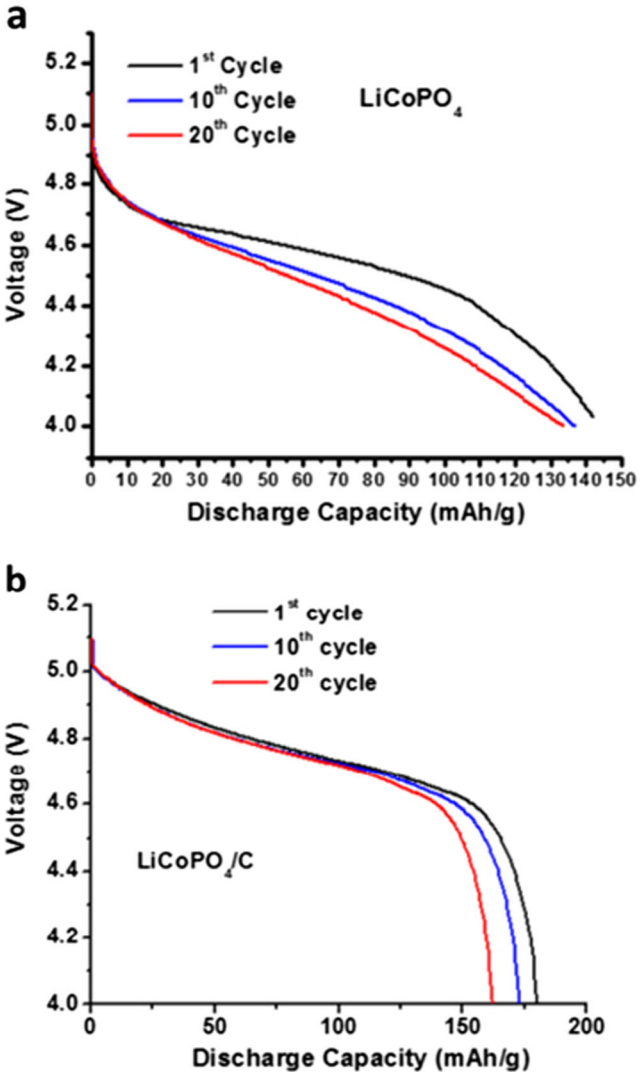

Fig. 7 Voltage versus discharge capacity plots of **a** pure and **b** carbon-coated $LiCoPO_4$ nanoparticles

images, the $LiCoPO_4$ sample has particle size distribution in the range 200–300 nm, and the average particle size of $LiNiPO_4$ nanoparticles is found to be 100 nm and noticed that the particles are agglomerated. The HRTEM image and EDS spectrum of carbon-coated $LiCoPO_4$ nanoparticles are shown in Fig. 5. Figure 5a has confirmed the formation of nanometer-scale thickness carbon layer uniformly on the surface of the $LiCoPO_4$ nanoparticles. Further, the EDS spectrum (Fig. 5b) has also confirmed the presence of Co, P, O, and C elements in the carbon-coated $LiCoPO_4$ sample. It is noteworthy to mention that the resin coating process is a cost-effective and simple way of coating carbon on the surface of the nanoparticles.

Transport number studies

The current versus time profile of the bare and carbon-coated $LiMPO_4$ (M = Co and Ni) nanoparticles is shown in Fig. 6. The transport numbers of ions and electrons for the bare and carbon-coated $LiCoPO_4$ nanoparticles are respectively found to be $t_i = 0.9602$ and $t_e = 0.0397$ and $t_i = 0.8921$ and $t_e = 0.1078$ (Fig. 6a, b). Similarly, the ionic and electronic transport numbers of bare and carbon-coated $LiNiPO_4$ nanoparticles have been obtained and found to be $t_i = 0.9821$ and $t_e = 0.0178$ and $t_i = 0.8641$ and $t_e = 0.1358$, respectively (Fig. 6c, d). These results indicate that the carbon-coated samples exhibited improved electronic conductivity in comparison with bare samples, which is due to the presence of carbon on the surface of the nanoparticles.

Electrochemical performance

The discharge profiles of bare and carbon-coated $LiCoPO_4$ nanoparticles, performed at 0.1 C, are shown in Fig. 7. From Fig. 7, it is observed that the bare and carbon-coated $LiCoPO_4$ nanoparticles exhibited typical voltage plateau at 4.83 V versus Li/Li^+, attributed to the $Co^{2+/3+}$ redox couple [27, 32]. The carbon-coated $LiCoPO_4$ delivered a first cycle discharge capacity of 180 mAh/g at the mid-point voltage of 4.76 V. The voltage characteristic for many batteries is such that the mid-point voltage is the approximate average voltage for the plateau of the discharge curve. This makes it possible to estimate an average performance in terms of voltage delivery to the load. The first cycle discharge capacities of bare and carbon-coated $LiCoPO_4$ nanoparticles are found to be 142 and 180 mAh/g, respectively. The carbon-coated $LiCoPO_4$ nanoparticles delivered 21 % higher discharge capacity as compared to bare sample and also higher than the theoretical capacity (167 mAh/g) of $LiCoPO_4$. The observed additional capacity may be due to the contribution from surface effect or other reasons which is to be probed. However, the cycling performance of both bare and carbon-coated $LiCoPO_4$ nanoparticle-based cells is found to decrease with cycle number, which may be due to the instability of the electrolyte at higher potentials [33]. As reported by Truong et al., $LiCoPO_4$ nanoparticles, nanorods, and nanoplates prepared by one-pot supercritical fluid method exhibited an initial discharge capacities of 105, 130, and 121 mAh/g, respectively, at 0.1 C rate [32]. In the present study, the prepared $LiCoPO_4$ nanoparticles exhibited higher discharge capacity (142 mAh/g) compared to these reported values.

Figure 8 shows the discharge curves of the bare and carbon-coated $LiNiPO_4$ nanoparticles at 0.1 C rate. From Fig. 8, it can be observed that both bare and carbon-coated $LiNiPO_4$ nanoparticles exhibit a voltage plateau at 5 V, corresponding to $Ni^{2+/3+}$ redox couple [34–36]. The initial discharge capacities of bare and carbon-coated $LiNiPO_4$ nanoparticles are 72 and 97 mAh/g, respectively. It indicates that the carbon-coated $LiNiPO_4$ nanoparticles exhibited 25.8 % higher discharge capacity as compared to bare $LiNiPO_4$. Further, the capacity fading is observed with cycling due to

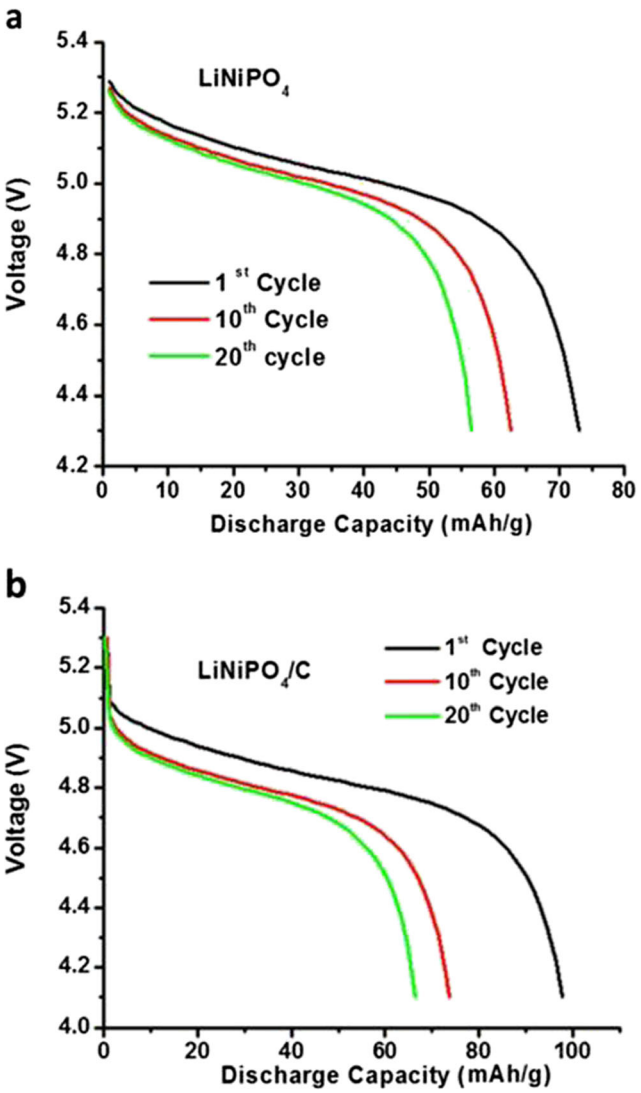

Fig. 8 Voltage versus discharge capacity plots for the **a** pure and **b** carbon-coated $LiNiPO_4$ nanoparticles

instability of electrolyte in the studied potential range [33]. The observed initial discharge capacities of bare and carbon-coated $LiNiPO_4$ nanoparticles are higher than the recently reported values [36].

The cycle life of bare and carbon-coated $LiMPO_4$ (M = Co and Ni) nanoparticle cathode-based lithium-ion cells has been presented in Fig. 9. From Fig. 9a, the discharge capacity of bare $LiCoPO_4$ cathode can be calculated as 142 and 133 mAh/g at the 1st and 20th cycles. The capacity retention after the 20th cycle is 93.6 %, whereas for the carbon-coated $LiCoPO_4$ nanoparticles, the capacity retention is 90 %. As observed from Fig. 9b, the capacity retention value for bare $LiNiPO_4$ nanoparticles is 76.3 % after the 20 cycle (the 1st cycle discharge capacity is 72 mAh/g and 20th cycle discharge capacity is 55 mAh/g for the bare $LiNiPO_4$). The discharge capacities are found to be 97 and 69 mAh/g, respectively, for the 1st and 20th cycle of the cells with carbon-coated $LiNiPO_4$ nanoparticles, and the capacity retention is 71.1 %. The electrical test results suggest that the carbon-coated $LiMPO_4$ (M = Co and Ni) nanoparticles exhibited an increased capacity as compared to bare samples, and also, it is observed that the bare and carbon-coated $LiMPO_4$ (M = Co and Ni) nanoparticles exhibited good cycle ability in the studied cycles. The superior electrochemical performance of carbon-coated $LiMPO_4$ (M = Co and Ni) nanoparticles is attributed to the presence of carbon on the surface of nanoparticles, which enhances the electron kinetics of the electrode.

The high discharge capacity and good cycle ability of the carbon-coated $LiMPO_4$ (M = Co and Ni) samples may be attributed to the nanoscale particle size and also the presence of conductive carbon on the surface of the particle, which facilitate better kinetic properties in Li-ion batteries. Generally, in lithium-ion batteries, both electrons and Li-ion transfer take place during charge-discharge process. A schematic representation of the electrons and Li-ion transport through the carbon-coated nanoparticles is shown in Fig. 10. As shown in Fig. 10, the nanosize particles provide shorter diffusion lengths and enhance the lithium-ion transport. The total surface area of nanoparticles increases the contact area with electrolyte and enables the rapid transport of lithium ions [2]. The electron transfer takes place through the grain boundaries, and the conductive carbon on the particle surface enhances the electron kinetics, and similar electrochemical performance of the carbon-coated $LiMnPO_4$ nanorods has been reported [2, 28]. The improved kinetic properties of electrons

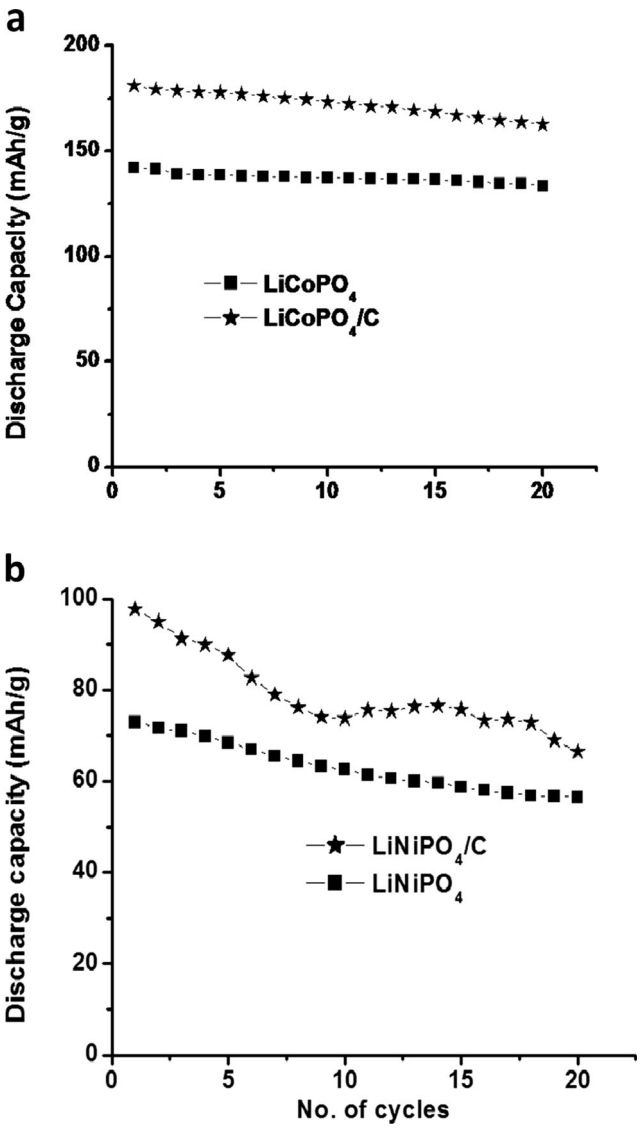

Fig. 9 Discharge capacity versus cycle number plots of **a** pure and carbon-coated $LiCoPO_4$ and **b** pure and carbon-coated $LiNiPO_4$ nanoparticles

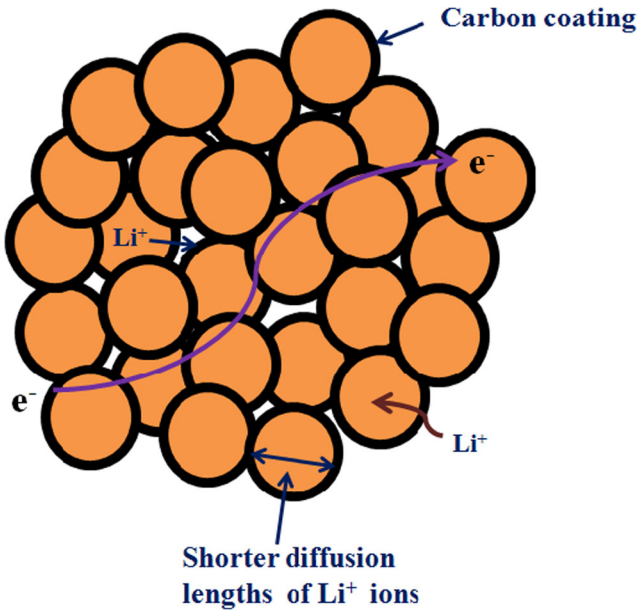

Fig. 10 Schematic representation of electrons and lithium-ion transport mechanism in carbon-coated $LiCoPO_4$/$LiNiPO_4$ cathode electrode

and Li-ions are responsible for good electrochemical performance in the case of the carbon-coated $LiMPO_4$ (M = Co and Ni) and suggest that these high potential cathode materials are suitable cathode for advanced lithium-ion batteries.

Conclusions

The bare and carbon-coated $LiMPO_4$ (M = Co and Ni) nanoparticles have been synthesized by the polyol method and the resin coating process, respectively. Structural and morphological studies respectively showed the purity of the phase and particle size of the $LiMPO_4$ (M = Co and Ni) systems. The TEM-EDS studies confirmed the formation of thin carbon layer uniformly over $LiCoPO_4$ nanoparticles. The carbon-coated $LiCoPO_4$ (180 mAh/g) and $LiNiPO_4$ (97 mAh/g) nanoparticles have exhibited an improved discharge capacities compared to bare samples, and it has been attributed to the presence of conducting carbon on the surface of the nanoparticles. The electron transport number (t_e) is also high for carbon-coated $LiMPO_4$ (M = Co and Ni) samples in comparison with bare samples, indicating an improved kinetic property of electrons which is responsible for good electrochemical performance. The carbon-coated $LiMPO_4$ (M = Co and Ni) nanoparticles can be promoted as a high potential cathode materials for high-power Li-ion batteries.

References

1. Valvo M, Lindgren F, Lafont U, Björefors F, Edström K (2014) Towards more sustainable negative electrodes in na-ion batteries via nanostructured iron oxide. J Power Sources 245:967–978
2. Nageswara Rao B, Ramesh Kumar P, Padmaraj O, Venkateswarlu M, Satyanarayana N (2015) Rapid microwave assisted hydrothermal synthesis of porous α-Fe_2O_3 nanostructures as stable and high capacity negative electrode for lithium and sodium ion batteries. RSC Advances 5:34761–34768
3. Jing S, Wu X-L, Yang C-P, Lee J-S, Kim J, Guo Y-G (2012) Self-Assembled $LiFePO_4$/C Nano/Microspheres by Using Phytic Acid as Phosphorus Source. J Phys Chem C 116:5019–5024
4. Fisher CAJ, Hart Prieto VM, Islam SM (2008) Lithium battery materials $LiMPO_4$ (M) Mn, Fe, Co, and Ni): insights into defect association, transport mechanisms, and doping behavior. Chem Mater 20:5907–5915
5. Howard WF, Spotnitz RM (2007) Theoretical evaluation of high-energy lithium metal phosphate cathode materials in li-ion batteries. J Power Sources 165:887–891
6. Wolfenstine J, Allen J (2004) $LiNiPO_4$–$LiCoPO_4$ solid solutions as cathodes. J Power Sources 136:150–153
7. Malik R, Burch D, Bazant M, Ceder G (2010) Particle size dependence of the ionic diffusivity. Nano Lett 10:4123–4127
8. Yang JS, Xu JJ (2006) Synthesis and characterization of carbon-coated lithium transition metal phosphates $LiMPO_4$ (M = Fe, Mn, Co, Ni) prepared via a nonaqueous sol-gel route. J Electrochem Soc 153:A716–A723
9. Choi D, Wang D, Bae IT, Xiao J, Nie Z, Wang W, Viswanathan VV, Lee YJ, Zhang JG, Graff GL, Yang Z, Liu J (2010) $LiMnPO_4$ nanoplate grown via solid-state reaction in molten hydrocarbon for li-ion battery cathode. Nano Lett 10:2799–2805
10. Oh SM, Oh SW, Yoon CS, Scrosati B, Amine K, Sun YK (2010) High-performance carbon-$LiMnPO_4$ nanocomposite cathode for lithium batteries. Adv Funct Mater 20:3260–3265
11. Nageswara Rao B, Venkateswarlu M, Satyanarayana N (2014) Structural, electrical and dielectric studies of nanocrystalline $LiMnPO_4$ particles. Ionics 20:927–934
12. Nageswara Rao B, Padmaraj O, Narsimulu D, Venkateswarlu M, Satyanarayana N (2015) A.C conductivity and dielectric properties of spinel $LiMn_2O_4$ nanorods. Ceram Int 41:14070–14077
13. Padhi AK, Nanjundaswamy KS, Goodenough JB (1997) Phospho-olivines as positive electrode materials for rechargeable lithium batteries. J Electrochem Soc 144:1188–1194
14. Chung SY, Bloking JT, Chiang YM (2002) Electronically conductive phospho-olivines as lithium storage electrodes. Nat Mater 2: 123–128
15. Herle PS, Ellis B, Nazar LF (2004) Nano-network electronic conduction in iron and nickel olivine phosphates. Nat Mater 3:147–152
16. Morgan D, VAN DER Van A, Ceder G (2004) Li conductivity in $LiMPO_4$ (M = Mn, Fe, Co, Ni) olivine materials. Electrochem Solid-State Lett 7:A30–A32
17. Ravet N, Chouinard Y, Magnan JF, Besner S, Gauthier M, Armand M (2001) Electroactivity of natural and synthetic triphylite. J Power Sources 97-98:503–507
18. Vadivel Murugan A, Muraliganth T, Ferreira PJ, Manthiram A (2009) Dimensionally modulated single-crystalline $LiMPO_4$ (M = Mn, Fe, Co, and Ni) with nano-thumblike shapes for high-power energy storage. Inorg Chem 48:946–952
19. Muraliganth T, Vadivel Murugan A, Manthiram A (2008) Nanoscale networking of $LiFePO_4$ nanorods synthesized by a microwave-solvothermal route with carbon nanotubes for lithium ion batteries. J Mater Chem 18:5661–5668
20. Yamada A, Koizumi H, Nishimura SI, Sonoyama N, Kanno R, Yonemura M, Nakamura T, Kobayashi Y (2006) Room-temperature miscibility gap in $LiFePO_4$. Nat Mater 5:357–360
21. Yamada A, Chung SC, Hinokuma K (2001) Optimized $LiFePO_4$ for lithium battery cathodes. J Electrochem Soc 148:A224–A229
22. Franger S, Cras FL, Bourbon C, Rouault H (2003) Comparison between different $LiFePO_4$ synthesis routes and their influence on its physico-chemical properties. J Power Sources 119-121:252–257
23. Ellis B, Kan WH, Makahnouk WRM, Nazar LF (2007) Synthesis of nanocrystals and morphology control of hydrothermally prepared $LiFePO_4$. J Mater Chem 17:3248–3254
24. Wang Y, Wang J, Yang J, Nuli Y (2006) High-rate $LiFePO_4$ electrode material synthesized by a novel route from $FePO_4 4H_2O$. Adv Funct Mater 16:2135–2140
25. Ding J, Su Z, Zhang Y (2016) Two-step synthesis of nanocomposite LiFePO4/C cathode materials for lithium ion batteries. New J Chemistry. doi:10.1039/C5NJ02626A
26. Zhang Y, Pan Y, Liu J, Wang G, Cao D (2015) Synthesis and electrochemical studies of carbon-modified $LiNiPO_4$ as the cathode material of li-ion batteries. Chem Res Chin Univ 31:117–122
27. Rosenberg S, Hintennach A (2015) In situ carbon coated $LiCoPO_4$ synthesized via a microwave_assisted path1. Russ J Electrochem 51:305–309
28. Ramesh Kumar P, Venkateswarlu M, Misra M, Mohanty AK, Satyanarayana N (2011) Carbon coated $LiMnPO_4$ nanorods for lithium batteries. J Electrochem Soc 158:A227–A230
29. Chandra S (1981) Super ionic solids principles and applications. North Holland Publishing Company, Amsterdam
30. Prakash I, Muralidharan P, Nallamuthu N, Venkateswarlu M, Satyanarayana N (2007) Preparation and characterization of nanocrystallite size cuprous oxide. Mater Res Bull 42:1619–1624

31. Koleva V, Stoyanova R, Zhecheva E (2010) Nano-crystalline $LiMnPO_4$ prepared by a new phosphate–formate precursor method. Mater Chem Phys 121:370–377
32. Truong QD, Devaraju MK, Ganbe Y, Tomai T, Honma I (2014) Controlling the shape of $LiCoPO_4$ nanocrystals by supercritical fluid process for enhanced energy storage properties. Scientific Reports 4:3975(1-8)
33. Bramnik NN, Nikolowski K, Baehtz C, Bramnik KG, Ehrenberg H (2007) Phase transitions occurring upon lithium insertion − extraction of $LiCoPO_4$. Chem Mater 19:908–913
34. Wolfenstine J, Allen J (2005) Ni^{3+}/Ni^{2+} redox potential in $LiNiPO_4$. J Power Sources 142:389–390
35. Karthickprabhu S, Hirankumar G (2014) Electrochemical studies on $LiNi_{0.85}Zn_{0.15}PO_4$ cathode material synthesized by polyol method. Int J ChemTech Res 6(13):5256–5260
36. Ornek A, Bulut E, Can M (2015) Influence of gradual cobalt substitution on lithium nickel phosphate nano-scale composites for high voltage applications. Mater Charact 106:152–162